

Aus der Klinik für Augenheilkunde
Universitätsklinikum des Saarlandes, UKS, Homburg/Saar
(Direktor: Prof. Dr. Berthold Seitz)

**Routine donor tomography in the eye bank as a sterile screening
method for improved graft selection in corneal transplantation**

**(Routinemäßige Spender-Tomographie in der Hornhautbank als sterile Screening-Methode für
eine verbesserte Auswahl des Spendergewebes für die Hornhaut Verpflanzung)**

Dissertation zur Erlangung des Grades eines Doktors der Medizin

der Medizinischen Fakultät
der UNIVERSITÄT DES SAARLANDES
2019

vorgelegt von: Fatema Asi
geb. 05.07.1991 in Palästina

Table of Contents

List of Abbreviation	2
List of Figures	4
List of Tables.....	5
Abstract in English.....	6
Zusammenfassung in Deutsch.....	7
1. Background and Purpose.....	9
1.1. History of Corneal Transplantation	9
1.2. Transplantation procedures overview (Table 1 ⁽¹⁰⁾)	10
1.2.1. Penetrating keratoplasty (PKP).....	10
1.2.2. Lamellar corneal transplantation.....	10
1.2.2.1. Deep Anterior Lamellar Keratoplasty (DALK)	10
1.2.2.2 Endothelial keratoplasty (EK).....	11
1.3. Eye Banking	14
1.3.1. Corneal preservation and storage	15
1.3.1.1. Hypothermic storage	15
1.3.1.2. Organ culture preservation	16
1.3.2. Donor selection and tissue evaluation	17
1.4. Anterior segment optical coherence tomography (AS-OCT)	18
1.5. Study Purpose	19
2. Patients and Methods.....	20

2.1. Methods.....	20
2.2. Data Analysis.....	22
3. Results.....	25
4. Discussion.....	29
4.1. Modern Eye Banking.....	29
4.2. Detection of curvature abnormalities in the donor	30
4.3. Limitations of the present study	34
4.3. Conclusions.....	35
5. References	36
Acknowledgements.....	46
Curriculum vitae	47

List of Abbreviations	
AC	Anterior Chamber
AD	Anno Domini
ALK	Anterior Lamellar Keratoplasty
AS-OCT	Anterior Segment Optical Coherence Tomography
CCT	Central Corneal Thickness [μm]
CV	Coefficient of Variation (%)
D	Diameter
DALK	Deep Anterior Lamellar Keratoplasty
DED	Dry Eye Disease
DM	Descemet Membrane
DMEK	Descemet Membrane Endothelial Keratoplasty
DOG	Deutsche Ophthalmologische Gesellschaft
DSAEK	Descemet Stripping Automated Endothelial Keratoplasty
DSEK	Descemet Stripping Endothelial Keratoplasty
ECC	Endothelial Cell Count
ECD	Endothelial Cell Density [cells/mm^2]
EEBA	European Eye Bank Association
EEBAD	European Eye Bank Association Directory
EK	Endothelial Keratoplasty
HEPES	Hydroxy Ethyl Piperazine Ethane Sulfonic acid
Kf	Keratometer of the flat surface (dpt)
Ks	Keratometer of the steep surface (dpt)
LASIK	Laser In-Situ Keratomileusis
M	Mean

Max	Maximum
MEM	Minimum Essential Medium
Min	Minimum
N	Sample size
OCT	Optical Coherence Tomography
Pf	Power of the flat surface (dpt)
PKP	Penetrating Keratoplasty
PLK	Posterior Lamellar Keratoplasty
PMMA	Polymethyl Methacrylate
PRK	Photorefractive Keratectomy
Ps	Power of the steep surface (dpt)
PTK	Phototherapeutic Keratectomy
Ra	The anterior radius of curvature (mm)
Rf	The flat radius of curvature (mm)
ROI	Region Of Interest
Rp	The posterior radius of curvature (mm)
Rs	The steep radius of curvature (mm)
SD	Standard Deviation
SD-OCT	Spectral Domain-Optical Coherence Tomography
SMILE	Small Incision Lenticule Extraction
ss-SD-OCT	Swept Source-Spectral Domain-Optical Coherence Tomography
TD-OCT	Time Domain-Optical Coherence Tomography
TGFBI	Transforming Growth Factor Beta Induced

List of Figures

Figure 1: In 2017, the number of keratoplasties in Germany increased to 8062 (A Report of the DOG-Section Cornea and its Keratoplasty Registry 2018) **12**

Figure 2: Proportions for keratoplasty types in Germany in 2017 (A Report of the DOG-Section Cornea and its Keratoplasty Registry 2018) **13**

Figure 3: The number of harvested and preserved donor tissues in the LIONS Eye Bank has almost tripled since its foundation in 2000 **13**

Figure 4: In organ culture: corneal tissues preserved in medium 1 (arrow) for a maximum of four weeks **16**

Figure 5: Endothelial cells under specular microscopy, which must be minimum 2.000 cells/mm² to be accepted for transplantation (adapted and modified (50)) **17**

Figure 6: a) The corneal donor tissue contained in the culture flask and fixed by the holder; b) The culture flask placed in a special holder to stabilize the donor cornea during the measurement **20**

Figure 7: The CASIA anterior segment-optical coherence tomography (AS-OCT) device..... **21**

Figure 8: Schematic data analysis (adapted and modified (53)); CCT: central corneal thickness; D: diameter **22**

Figure 9: Region of interest (ROI) marked to eliminate the artifacts (adapted and modified (53)) **23**

Figure 10: Adaptation of a spherocylindrical surface model (arrow) (adapted and modified (53)) **23**

Figure 11: 3D volume data of the donor corneoscleral button within a 7.0 mm central zone (adapted and modified (91)) **24**

Figure 12: a) A construction drawing of the polymethyl methacrylate (PMMA) phantom; b) Central B-scan from a volumetric data set of the polymethyl methacrylate (PMMA) phantom (adapted and modified (91)) **25**

Figure 13: A videokeratoscope presented by Stoiber et al. as an evaluation method to screen the donor tissues (adapted and modified (107)) **31**

List of Tables

Table 1: Corneal transplantation procedures, their indications, and major complications (adapted and modified (10)) **14**

Table 2: Manufacturer's instructions of the polymethyl methacrylate (PMMA) phantom and measurement results for the phantom contained in a culture medium flask (adapted and modified (53)) (Ra = anterior surface radius of curvature, Rp = posterior surface radius of curvature, Rs = the steep radius of curvature, Rf = the flat radius of curvature, CCT = central corneal thickness) **25**

Table 3: The mean (M), standard deviation (SD), maximum (Max), minimum (Min), and coefficient of variation (CV) for each measurement..... **26**

Table 4: Comparison between the standard eye values according Gullstrand's model eye in literature to the average measurements of the 200 donor corneas (we presented the same comparison in a previous published study, but with a smaller sample size of 74 corneas (adapted and modified (53)) **27**

Table 5: Different variables with their confidence interval, the number of values outside the confidence interval, and their percentage of data sample (N) (N=200)..... **27**

Abstract in English

Purpose: To evaluate the efficiency of using anterior segment optical coherence tomography (AS-OCT) (CASIA2) as a non-invasive and sterile screening method in the eye bank to detect corneal grafts with curvature and/or thickness abnormalities, thus improving the graft selection for corneal transplantation.

Methods: Two hundred donor corneal tissues mounted in sterile tissue cultivation flasks were imaged using AS-OCT (CASIA 2). The corneal tissues were preserved at least 24 hours in medium 2 (6% dextran T-500) before the measurement. All images were grabbed through the posterior surface of the corneal tissues within a 7 mm central zone to create 3D volume data. The volume data set was imported to MATLAB and, after preprocessing the data and defining the region of interest (ROI), the edge of the front and back surfaces of the corneal tissues was detected. Subsequently, the adaptation of a sphero-cylindrical surface model with raytracing was carried out. The radii of curvature for the front and back surfaces and the central corneal thickness were determined according to the method proposed by Mäurer S., Eppig T., and Langenbucher A. at the Institute of Experimental Ophthalmology, Homburg/Saar.

Results: The mean steep/flat front surface radius was 7.5 ± 0.24 (6.6-7.9) / 7.7 ± 0.22 (7.1-8.8) mm, the corresponding values for the back surface being 6.6 ± 0.22 (5.9-7.1) / 6.8 ± 0.21 (6.2-7.5) mm and the mean central thickness was 582 ± 45.1 (453-693) μm . Abnormalities (beyond ± 2 SD) were found in 13 corneas (6.5%) for anterior surface curvature, 15 for corneas (7.5%) for the posterior surface, and five corneas (2.5%) for thickness.

Conclusions: The AS-OCT provides an objective and sterile. In addition, it may allow, in the future, a semi-automated screening method to identify corneal morphological and refractive alterations (e.g., keratoconus, status post PRK/LASIK) to further optimize corneal donor selection in eye banks.

Zusammenfassung in Deutsch

Ziel: Bewertung der Effizienz der optischen Kohärenztomographie des vorderen Augenabschnitts (AS-OCT) (CASIA2) als nicht-invasive und sterile Screeningsmethode in der Hornhautbank zur Erkennung von Hornhauttransplantaten mit Krümmungs- und/oder Dickenanomalien, wodurch die Transplantatauswahl für die Hornhauttransplantation verbessert werden sollte.

Methoden: 200 Spenderhornhautgewebe wurden im sterilen Gewebekultivierungsbehälter vermessen. Die Hornhautgewebe wurden mindestens 24 Stunden vor der Messung in Medium 2 (mit 6% Dextran T-500) konserviert. Alle Bilder wurden durch die hintere Oberfläche der Hornhautgewebe innerhalb einer zentralen Zone von 7 mm aufgenommen, um 3D-Volumendaten zu erstellen. Der Volumendatensatz wurde in MATLAB importiert, und nach der Vorverarbeitung der Daten und der Definition der "Region of interest" (ROI) wurde die Kante der Vorder- und Rückseite der Hornhautgewebe detektiert. Anschließend erfolgte die Anpassung eines sphärozyylinderförmigen Oberflächenmodells mittels Raytracing. Die Krümmungsradien für Vorder- und Rückseite sowie die Dicke der zentralen Hornhaut wurden nach der von Mäurer S, Eppig T und Langenbacher A (Institut für Experimentelle Ophthalmologie, Homburg/Saar) vorgeschlagenen Methode bestimmt.

Ergebnisse: Der mittlere steile / flache Radius der Vorderfläche betrug $7,5 \pm 0,24$ (6,6-7,9) / $7,7 \pm 0,22$ (7,1-8,8) mm, die entsprechenden Werte für die Rückfläche betragen $6,6 \pm 0,22$ (5,9-7,1) / $6,8 \pm 0,21$ (6,2-7,5) mm und die mittlere zentrale Dicke betrug $582 \pm 45,1$ (453-693) μm . Anomalien (außerhalb ± 2 SD) wurden bei 13 Hornhäuten (6,5%) für die Krümmung der Vorderfläche, bei 15 Hornhäuten (7,5%) für die Krümmung der hinteren Oberfläche und bei 5 Hornhäuten (2,5%) für die zentrale Dicke gefunden.

Schlussfolgerungen: Das Vorderabschnittes-OCT bietet eine objektive, sterile und zukünftig halbautomatisches Screening-Methode zur Identifizierung morphologischer und refraktiver Veränderungen der Hornhaut (z. B. Keratokonus, Status nach PRK/LASIK), um die Hornhautspenderauswahl in der Hornhautbank weiter zu optimieren.

1. Background and Purpose

The cornea is the clear front surface of the eye. It lies directly in front of the iris and pupil, and it allows light to enter the eye. It accounts for approximately two-thirds of the eye's total optical power (1).

Anatomically, the human cornea has five layers (from anterior to posterior) (1):

- The corneal epithelium
- Bowman's layer
- The corneal stroma
- Descemet's membrane
- The corneal endothelium

The clarity of the cornea depends on its state of dehydration, the vascularity, and the uniformity of its structure. If the cornea becomes damaged through disease, infection, or injury, this can cause scarring, opacification, corneal irregularity, and, subsequently, reduced vision.

However, the treatment of corneal diseases depends on many factors and has a wide spectrum, which can lead to corneal transplantation, in which the diseased cornea is replaced with a healthy donor transplant to restore vision (1).

1.1. History of Corneal Transplantation

The history of corneal transplantation dates to over two centuries with experiments using allografts and xenografts by inspired individuals. The original concept of corneal surgery dates to the Greek physician Galen (130-200 AD) (1-2). In 1905, Eduard Konrad Zirm, in Olmütz near Prague, performed the first successful corneal transplant, which was the beginning of a long line of corneal transplantation research and techniques (3).

Vladimir Filatov, a Russian ophthalmologist, played an obvious role in developing a new method for full-thickness keratoplasty in the 1920s and 1930s. He was the first to suggest using cadaver corneas for penetrating keratoplasty (PKP) in the 1930s (4, 5). This idea was further developed by the American ophthalmologist Richard Paton (6).

During his research fellowship in the United States, the Spanish ophthalmologist Ramon Castroviejo developed a double-bladed knife for square grafts and suggested using direct sutures, which was responsible for popularizing PKP in the United States in the 1930s (7-8).

Many important medical advances, such as the introduction of antibiotics in the 1940s, the development of microsurgical techniques and instruments in the 1950s, and the use of steroids in the 1970s, as well as advances in corneal preservation and eye banking led to more successful corneal surgeries (8). PKP has traditionally been the treatment of choice for corneal opacifications.

Over the last 20 years, new anterior and posterior lamellar techniques have become available that selectively replace only the cornea's diseased layers while retaining healthy layers.

1.2. Transplantation procedures overview (Table 1 ⁽¹⁰⁾)

1.2.1. Penetrating keratoplasty (PKP)

PKP is a full-thickness transplant procedure, in which a trephine of an appropriate diameter is used to make a full-thickness resection of the patient's cornea, followed by placement of a full-thickness donor corneal graft (9). PKP is indicated in keratoconus, full-thickness corneal scars, graft replacement after prior graft failure, Fuchs' endothelial dystrophy combined with longstanding endothelial-epithelial decompensation with stroma scars, pseudophakic or aphakic bullous keratopathy, infection, and trauma (Table 1) (9-11).

1.2.2. Lamellar corneal transplantation

Selective lamellar keratoplasty describes procedures that selectively replace only diseased layers, resulting in improved visual outcomes and reduced complications (Table 1) (11-12).

1.2.2.1. Deep anterior lamellar keratoplasty (DALK)

DALK is a partial-thickness corneal transplantation that involves only the donor stroma, leaving the recipient's own Descemet's membrane (DM) and endothelium intact. DALK is

most useful for treating corneal pathologies in circumstances of a normally functioning endothelium (Table 1) (12-14).

Some indications could be treated by anterior lamellar keratoplasty (ALK), mainly deep anterior lamellar keratoplasty (DALK), including corneal pathologies with intact endothelia and intact Descemet's membranes (DMs) (12):

- Keratoconus
- Stromal dystrophies without endothelial involvement (e.g., Schnyder corneal dystrophy)
- Epithelial-stromal TGFBI dystrophies (e.g., granular and lattice dystrophies), especially after unsuccessful phototherapeutic keratectomy (PTK) (15).

1.2.2.2 Endothelial keratoplasty (EK)

Posterior lamellar keratoplasty (PLK), which comprises partial corneal transplantation of the posterior cornea, has developed significantly over the past two decades to become a suitable alternative to PKP in the management of endothelial dysfunction, but extensive time and experience was required to develop a reliable surgical PLK technique.

Tillet performed the first PLK in 1956 (16). This is considered to be the first case to depend on the concept of selective replacement of diseased posterior corneal tissue. In 1964 and 1980, Polack and Jose Barraquer, respectively, described new endokeratoplasty techniques with some modifications (17-18). Because of the difficulty of the techniques and limited clinical success, each of these techniques had significant drawbacks until major developments in the past two decades.

Dr. Gerrit Melles laid the foundation for modern EK (19). In 1998, he was the first to suggest that a posterior graft could be placed on recipient stroma without sutures, calling it "posterior lamellar keratoplasty." In this procedure, the anterior stroma was left intact and a deep stromal pocket (depth ~50%) was created across the cornea through a superior scleral incision (20-23). This technique was adopted, modified, and popularized by Price et al. as 'Descemet stripping automated endothelial keratoplasty' (DSAEK) (24). DSAEK has been considered a reliable surgical PLK technique for a long time, especially in the United States (25).

Another modification of EK, also suggested by Melles, was to transplant only donor DM and endothelial cells without stromal tissue (19). This procedure is referred to as Descemet membrane endothelial keratoplasty (DMEK) (19).

*** Statistically overview in Germany:**

- In 2017, the number of keratoplasties in Germany increased to 8052 (Figure. 1).
- The “German Keratoplasty Registry,” which was established by the Cornea Section of the German Ophthalmological Society (Deutsche Ophthalmologische Gesellschaft DOG) in 2000, reported the following proportions for keratoplasty in Germany in 2017 (Figure. 2) (26):
 - 38.4% for PKP
 - 58.6% for PLK
 - 3.0% for ALK
- Further, the number of keratoplasties in Homburg/Saar (542 has increased approximately eight-fold over the last 12 years and the number of harvested and preserved donor tissues in our LIONS eye bank has almost tripled (560 in 2017) since its founding in 2000 (Figure. 3) (26).

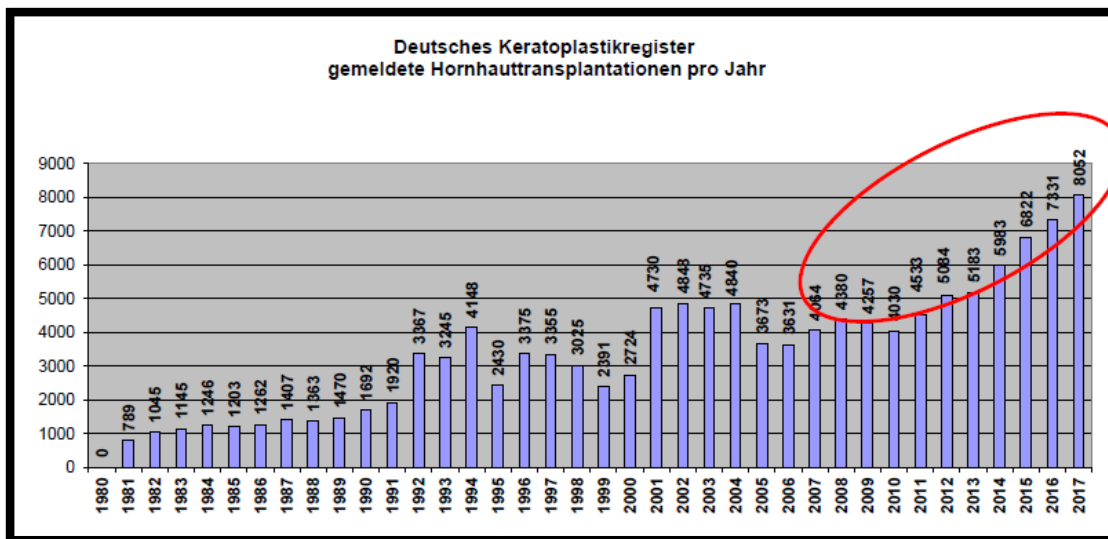


Figure 1: In 2017, the number of keratoplasties in Germany increased to 8062 (A Report of the DOG-Section Cornea and its Keratoplasty Registry 2018)

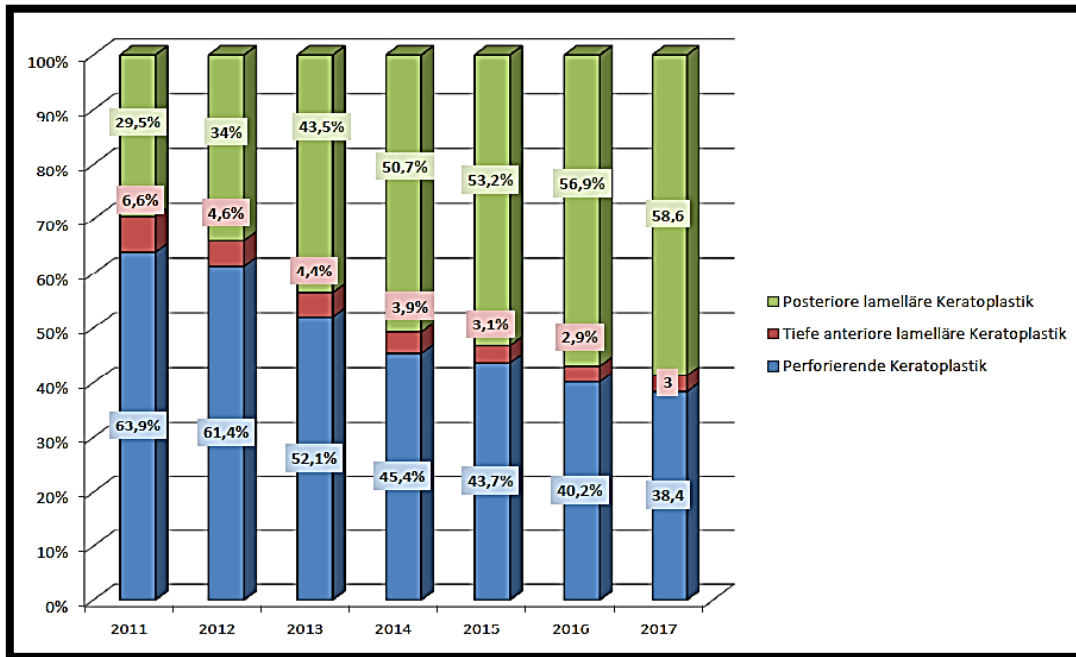


Figure 2: Proportions for keratoplasty types in Germany in 2017 (A Report of the DOG-Section Cornea and its Keratoplasty Registry 2018)

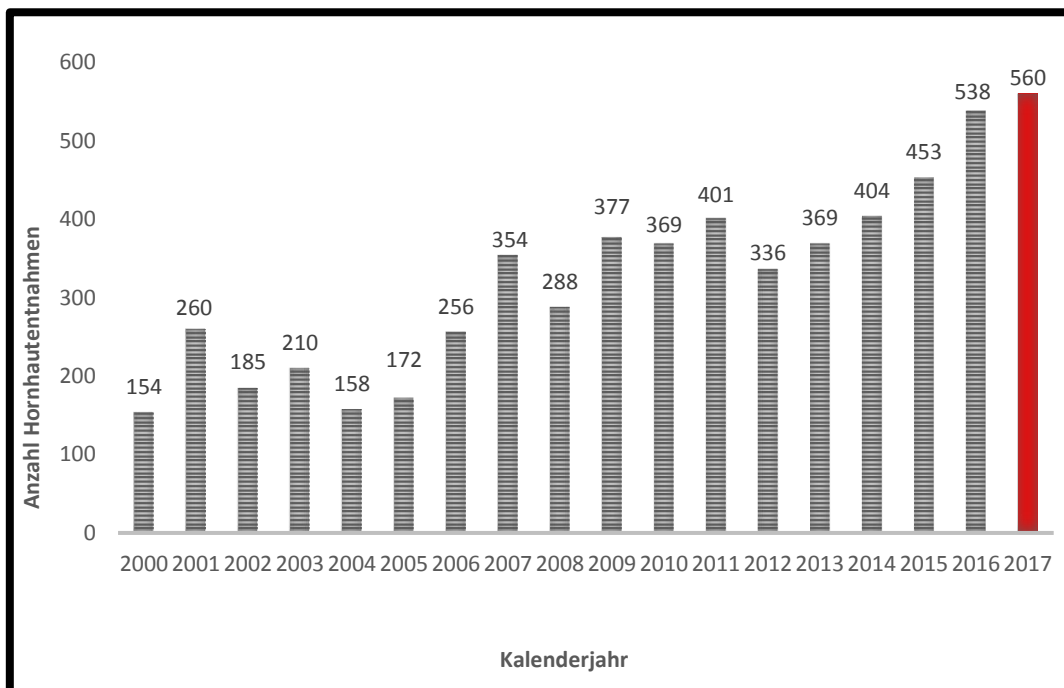


Figure 3: The number of harvested and preserved donor tissues in the LIONS Eye Bank has almost tripled since its foundation in 2000

Table 1: Corneal transplantation procedures, their indications, and major complications (adapted and modified (10))

	PKP	DALK	DSAEK	DMEK
Surgery	The diseased host cornea is replaced completely Full-thickness donor graft	The diseased host epithelium and stroma are replaced Donor cornea epithelium, Bowman’s layer, and corneal stroma	The diseased host endothelium and DM are replaced Donor endothelium, DM, and stroma	The diseased host endothelium and DM are replaced Donor endothelium and DM
Common indications	Full-thickness scar, bullous keratopathy with stromal scars, keratoconus with rupture of Descemet’s membrane and graft failure	Keratoconus, stromal scar, hereditary stromal dystrophies without endothelial involvement	Fuchs’ dystrophy, bullous keratopathy and graft failure with good curvature and unknown stromal scars	Fuchs’ dystrophy, bullous keratopathy and graft failure with good curvature and unknown stromal scars
Major complications	Graft rejection, graft failure, expulsive hemorrhage, infection, astigmatism and suture complications	Graft rejection, intraoperative DM tear, astigmatism	Graft detachment, graft failure, and graft rejection	Graft detachment, graft failure, and graft rejection (1-3%)

1.3. Eye Banking

Eye banks are the main key to helping surgeons get the best-preserved corneal transplants. They play an important role in preserving and preparing ocular tissues, which can be used for surgical purposes. Moreover, they can be used for research goals to develop and discover new treatment options and methods in corneal transplantation (27).

As mentioned above, the first successful full-thickness corneal transplantation was performed in 1905 (3, 28) when an 11-year-old donor patient who had a fragment of iron in his eye

following trauma had undergone therapeutic enucleation. Early corneal transplants relied on tissue from live donors. Therefore, the enucleated eye was preserved in warm saline at the temperature of the human body and corneal transplantation was performed with minimum delay on the same day of harvesting (i.e., within six hours) (29).

It was not until the 1930s that using corneas from deceased donors and the storage of whole eyes in glass pots (moist chambers) on ice for several days was pioneered (29). The first eye bank was established in New York in the 1940s (27, 30).

1.3.1. Corneal preservation and storage

After many developments in surgical tools, procedures, and antibiotic and corticosteroid use in the 1950s, the success rate of corneal transplantation has increased (29). Consequently, the application of corneal transplantation and the need for donor grafts have increased. Therefore, besides the possibility of using eyes from human cadavers, many trials were made to improve and increase the storage time for cadavers' tissue with preserving the endothelial layer, which is important to maintain corneal clarity (29, 31, 32).

In the 1970s, two methods for storage of the excised corneoscleral buttons were introduced in the USA and are still applied: hypothermic storage (33, 34) and organ culture preservation (35-37). Cryopreservation was considered one of the approaches to preserve the donor corneas, but because of its complexity and the risk of damaging the corneal endothelium, its application was limited in routine eye banking, except for urgent transplants where the main purpose was to save the eye (38).

1.3.1.1. Hypothermic storage

In hypothermic storage, the cooling of tissues and organs reduces cellular demand for metabolic energy (39). Corneas are preserved at 4°C in a tissue culture medium that contains antibiotics and dehydrating agents (dextran, chondroitin sulfate), to prevent corneal swelling (33, 34).

In the early 1970s, hypothermic storage of corneoscleral discs became the method of choice with the introduction of the McCarey-Kaufman medium (M-K medium) (30). The original M-K

medium (31) has been supplemented with solutions, such as in “K-sol,” “Dexsol,” and “Likorol,” potentially allowing for a 10-day preservation period, which was thought to be the maximum for the M-K medium (40). Hypothermic preservation times have been extended with the development of the Optisol-GS solution, which contains dextran and chondroitin sulfate, to reach a preservation time of 14 days (31, 39).

1.3.1.2. Organ culture preservation

The standard organ culture medium (Medium 1) consists of MEM-Earle’s supported with penicillin/streptomycin/amphotericin B, L-glutamine, HEPES buffer, and NaHCO₃. Corneas are incubated in organ culture media at 28–37°C. This medium allows for a 30-day preservation period without significant endothelial cell loss (41) (Figure 4).

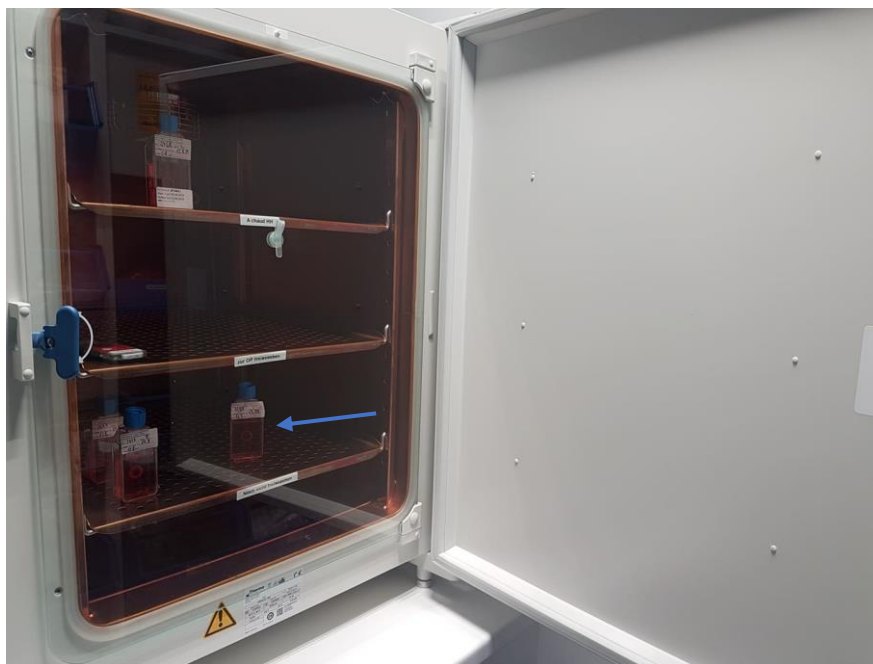


Figure 4: In organ culture: corneal tissues preserved in medium 1 (arrow) for a maximum of four weeks

However, because of the absence of dehydrating agents, the medium leads to a significant corneal swelling of up to 1000–1500 μm , which must be reversed during a 1-3 day deswelling period before transplantation. This is achieved by placing the graft in a “transport medium” (medium 2) composed of medium 1 plus an additional osmotic agent (typically 6% dextran T-500)—a hydrophilic macromolecule that produces colloid osmotic pressure and reduces

corneal thickness by extracting water from the stroma to achieve a corneal graft thickness similar to that of the recipient's cornea at the time of surgery (27, 42).

According to European Eye Bank Association Directory (EEBAD) (44), in 2010, 70% of corneas out of the 62 eye banks included in EEBAD were stored by organ culture.

DMEK was introduced in our department in 2012 and it was not clear which transport medium should be used. According to the guidelines for penetrating keratoplasty, a transport medium with dextran was used. However, this was changed according to Abdin et al. (44), who reported on the potential negative effect of dextran in the transport medium for pre-stripped tissue.

1.3.2. Donor selection and tissue evaluation

Donor selection depends on multiple variables, such as corneal clarity at slit lamp examination, endothelial cell density (ECD) and vitality, endothelial cell morphology, post-mortem time, and preservation time. Endothelial cell count (ECC) seems to decrease with time after corneal transplantation, which causes a risk of graft failure. Therefore, ECC is considered a key variable in the selection process and for keratoplasty success (45). Moreover, endothelial examination of donor corneas by light microscopy and ECC estimation are considered important quality indicators in determining the suitability of corneas for transplantation (46).

According to Armitage WJ et al., the change in ECD after corneal transplantation suggests a cornea with an ECD of $\geq 2,200$ cells/ mm^2 should have enough endothelial cells to maintain corneal transparency for at least 25 years (47, 48) (Figure 5).

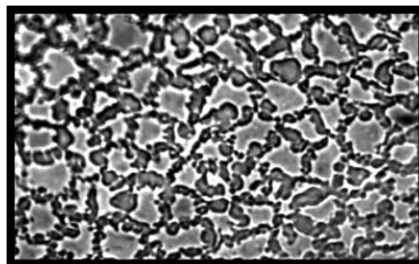


Figure 5: Endothelial cells under specular microscopy, which must be minimum 2.000 cells/ mm^2 to be accepted for transplantation (adapted and modified (50))

Donor corneas should be evaluated by light microscopy in combination with specular microscopy (49, 50). However, according to the 2016 Eye Bank Association of America's report, there are several reasons why tissue intended for surgery may not ultimately be used for surgery. 42.5% of donor corneas were not transplanted because of tissue suitability problems (per light microscopy and specular microscopy) and 17.4% of the tissue problems were because of the cornea stroma (51).

Each high-volume corneal transplant surgeon may have inadvertently grafted donor cornea with keratoconus or state post refractive surgery, resulting typically in major patient disadvantages.

Thus, tomographic screening using a clinical optical coherence tomography (OCT) device could be used to avoid refractive surprises for patients and microsurgeons after keratoplasty (52).

1.4. Anterior segment optical coherence tomography (AS-OCT)

OCT was first developed by Huang et al. (53, 54). It is a noncontact optical signal acquisition and processing technique that provides magnified, high-resolution, cross-sectional images of ocular tissues using low-coherence interferometry (55, 56, 57). Currently, there are two different platforms from the OCT device: time domain (TD-OCT) and spectral domain (SD-OCT) (58).

AS-OCT was introduced in 1994 and was available for routine clinical use in 2001 (60, 61). It offers several advantages: it is sterile, noncontact, and generates high-resolution cross-sectional images of the tissues in a short time (57, 61). Moreover, it is helpful in diagnosing and managing anterior segment diseases, planning and performing surgery, monitoring postoperative courses, and research purposes (62, 63):

- Conjunctival diseases: pterygium and pinguecula, melanoma or nevi (64, 65, 66).
- Anterior segment-tumors: SD-OCT shows hyperreflective, thickened epithelium with abrupt transitions from normal to abnormal epithelium (67). It is helpful in diagnosing Salzmann nodular degeneration and iris and ciliary tumors (68, 69).
- Corneal diseases: microbial keratitis, acute hydrops (70-72), corneal scars (73). According to Agarwal A. et al. (74), AS-OCT can be used to detect AC inflammation in cases of decreased corneal clarity and corneal edema.

- Dry eye diseases (DED): AS-OCT is a reliable method for diagnosing and following up on DED by quantitative evaluation of tear film thickness and tear film meniscus (75-79)
- Anterior segment trauma: it offers a high-resolution image that can be used to determine the depth of the injury to the cornea or sclera, and the type, size, and location of foreign bodies (80, 81).
- Anterior segment surgery: cataract surgery for preoperative calculation of lens power, especially in patients with a history of refractive surgery, evaluation of AC, and risk factors for postoperative complications (82, 83). It is used in corneal transplantation for preoperative and postoperative graft evaluation (84, 85) and for refractive surgery by enabling an accurate measurement laser in situ keratomileusis (LASIK) flap thickness and residual stroma thickness preoperative to avoid postoperative ectasia (86, 87, 88).
- Assessment of anterior segment biometry: for example, corneal thickness changes caused by contact lens wear, evaluation of AC dimensions (89, 90).

1.5. Study Purpose

To evaluate the efficiency of using anterior segment optical coherence tomography (AS-OCT) (CASIA2) as a non-invasive and sterile screening method to detect corneal grafts with curvature and/or thickness abnormalities before corneal transplantation.

2. Patients and Methods

2.1. Methods

Two hundred donor corneal tissues mounted in sterile tissue cultivation flasks were imaged using AS-OCT CASIA 2 (Tomey Corp., Nagoya, Japan) in this *prospective* study.

The 200 corneal donor tissues were preserved in the LIONS eye bank (Department of Ophthalmology, Saarland University Medical Center) according the standard guidelines of the European Eye Bank Association (EEBA).

The measurement was carried out 24 to 30 hours after being transferred to the deswelling medium, which contained 6% dextran T-500 (medium 2) at room temperature. Each measurement lasted for about two minutes. The culture flask was positioned in a holder on the chin rest of the OCT device using a 3D printer (Ultimaker 2 Go, Ultimaker B.V., Geldermalsen, The Netherlands) to fixate the cornea during the measurement (91) (Figure 6).

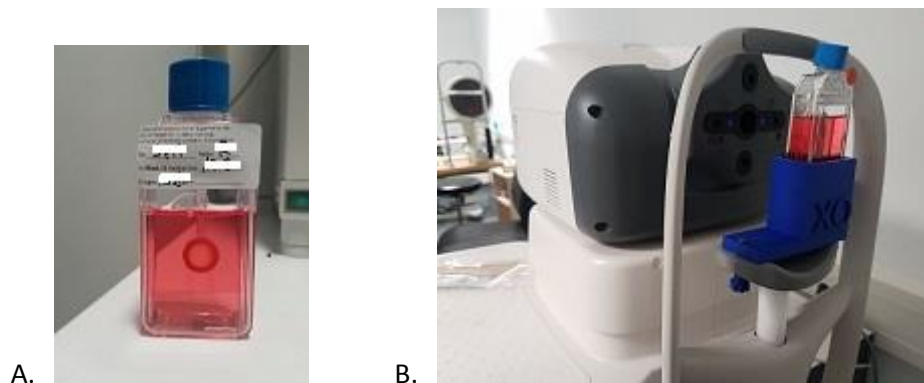


Figure 6: a) The corneal donor tissue contained in the culture flask and fixed by the holder; b) The culture flask placed in a special holder to stabilize the donor cornea during the measurement

Subsequently, the donor corneas were imaged from different angles through the back surface of the donor cornea and then the raw data was imported into MATLAB (The MathWorks Inc., Natick, USA) to be analyzed and to create a 3D volume set.

In this study, we used an ss-SD-OCT system (swept-source OCT), CASIA 2, with a central wavelength of $\lambda = 1310$ nm that allows for a penetration depth of up to 13 mm in vivo (23), which is sufficient to represent the donor cornea within the bottle (92) (Figure 7).

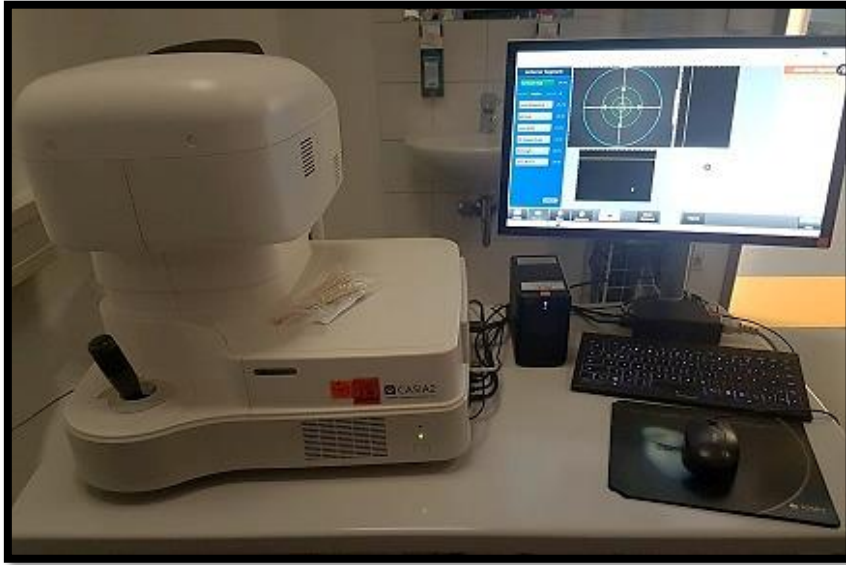


Figure 7: The CASIA anterior segment-optical coherence tomography (AS-OCT) device

2.2. Data Analysis

We proposed the data analysis in a previous published article (Mäurer S, Asi F, Rawer A, Damian A, Seitz B, Langenbucher A, Timo Eppig. [Concept for 3D measurement of corneal donor tissue using a clinical OCT]. *Ophthalmologe* 2019;116:640-646 (53).

After imaging the donor corneas from the posterior surface, the raw data was imported into MATLAB (The MathWorks Inc., Natick, USA) and analyzed according to the scheme shown in Figure 8. First, the image data was preprocessed. The basics of image preprocessing have already been presented by Damian et al. (52). Subsequently, a spherocylindrical surface model was adapted to the segmented surfaces and, finally, the central corneal thickness was determined.

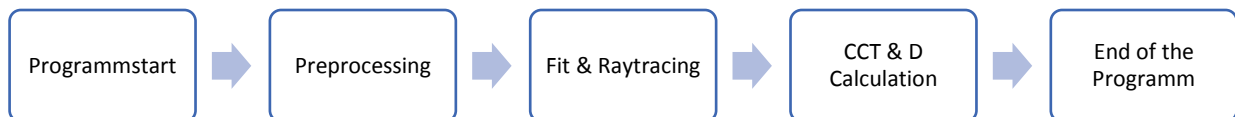


Figure 8: Schematic data analysis (adapted and modified (53)); CCT: central corneal thickness; D: diameter

The preprocessing step consists of removing artifacts created by the holder by defining a region of interest (ROI) that would hide artifacts. Subsequently, filters were used to remove the images of small particles and background noise and to detect the edge of the leading and trailing edges of the cornea (Figure 9) (90).

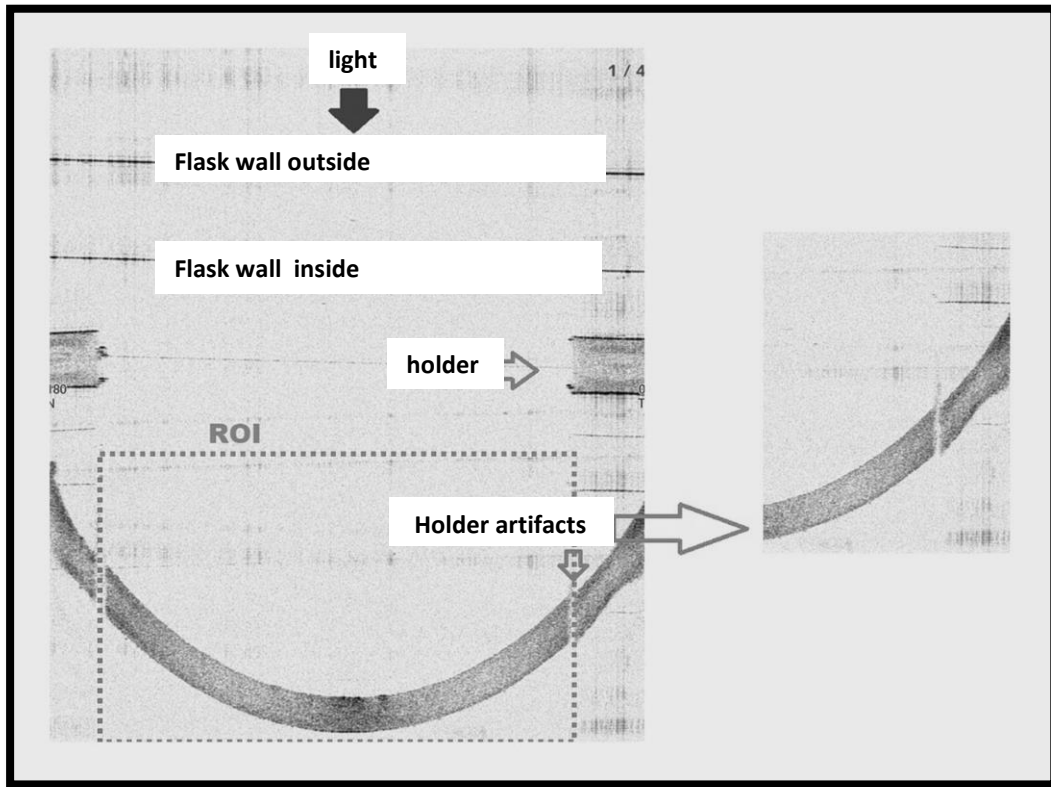


Figure 9: Region of interest (ROI) marked to eliminate the artifacts (adapted and modified (53))

After the preprocessing, the adaptation of a sphero-cylindrical surface model (Figure 10) with raytracing was completed (53).

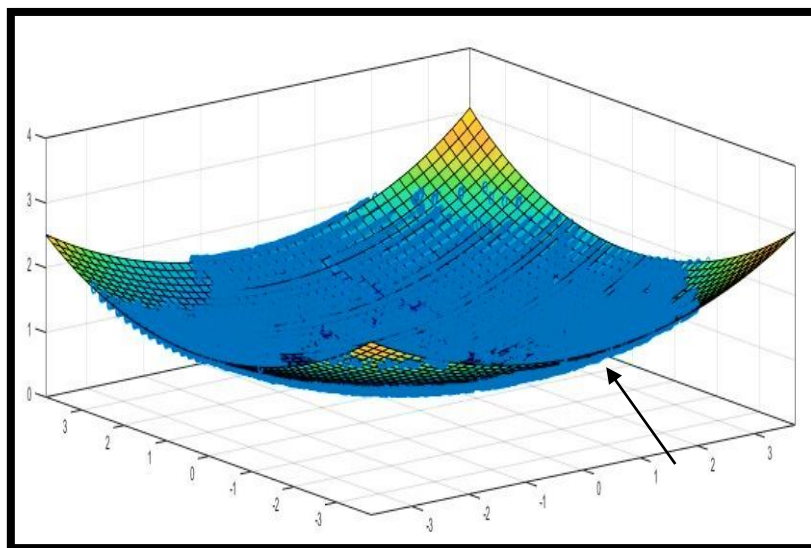


Figure 10: Adaptation of a spherocylindrical surface model (arrow) (adapted and modified (53))

As the storage and position of the donor tissues in the cell culture flasks is not identical for each sample, the sample translation was first taken by considering the displacement of the apex from the zero point of the coordinate system in space (53).

3D volume data of the donor corneoscleral button within a 7.0 mm central zone were grabbed using a raster scan through the cornea's posterior surface (Figure 11) (53).

By creating two surface models for the front and back surfaces, geometric characteristics of the donor cornea, such as the radii of curvature, the surface refractive indices, and the keratometer value were calculated (53). The central corneal thickness was determined from the distance of the anterior and posterior surfaces of the apex (53).

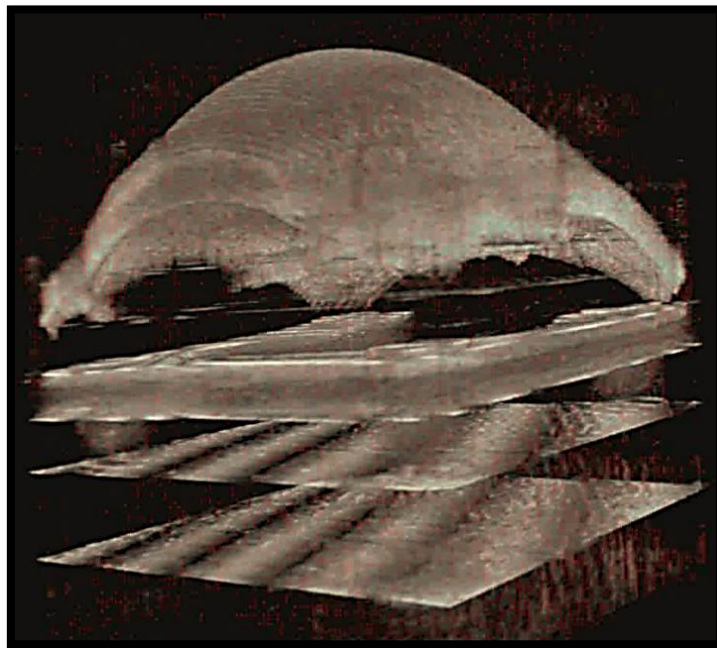


Figure 11: 3D volume data of the donor corneoscleral button within a 7.0 mm central zone (adapted and modified (91))

3. Results

To validate the MATLAB program, a polymethyl methacrylate (PMMA) Phantom was used in form of a cornea (Figure 12) with the OCT (54). In Figure 12, the central frame of the volume data set for the phantom is shown. This was subsequently evaluated with the program described above. The deviant refractive index of PMMA (a polymethyl methacrylate) ($n = 1.4820$ (93)) was considered (91).

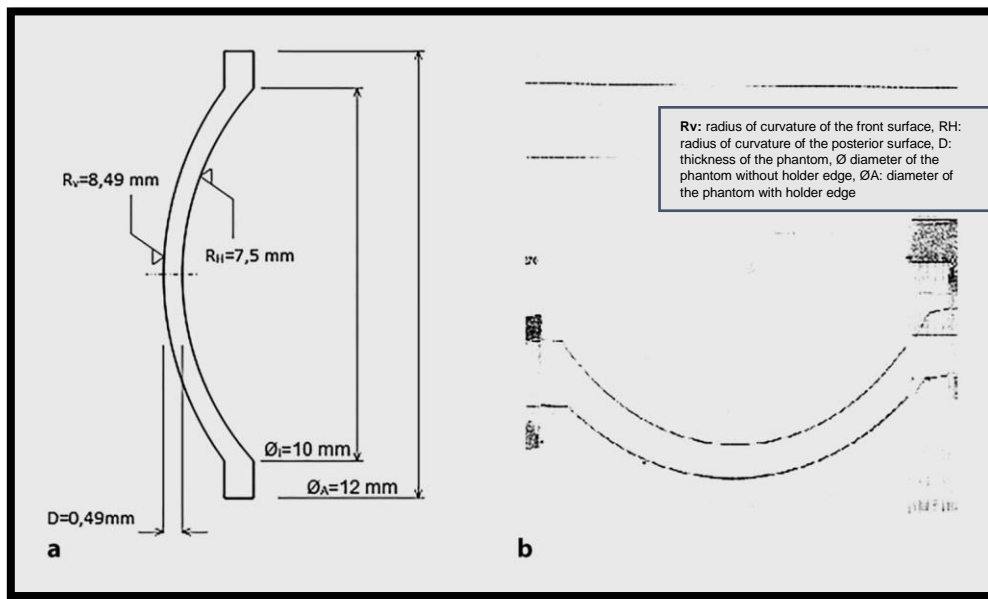


Figure 12: a) A drawing of the polymethyl methacrylate (PMMA) phantom; b) Central B-scan from a volumetric data set of the polymethyl methacrylate (PMMA) phantom (adapted and modified (91))

Table 2: Manufacturer's instructions of the polymethyl methacrylate (PMMA) phantom and measurement results for the phantom contained in a culture medium flask (adapted and modified (53))
(R_a = anterior surface radius of curvature, R_p = posterior surface radius of curvature, R_s = the steep radius of curvature, R_f = the flat radius of curvature, CCT = central corneal thickness)

	Manufacturer's instructions of the PMMA phantom	Measurement results for the phantom contained in a culture medium flask	
		The steep radius of curvature (R_s)	The flat radius of curvature (R_f)
Anterior surface radius of curvature (R_a) (mm)	8.49	8.13	8.13
Posterior surface radius of curvature (R_p) (mm)	7.5	7.44	7.39
Ra: Rp	1.13	1.1	1.1
CCT (μm)	490	499	

It is possible to measure and image the PMMA phantom and the donor cornea with AS-OCT as shown in Figure 12. The phantom is made from of an optical homogeneous material and, therefore, only the edges are sharp, and the phantom appears empty inside. On the other hand, the cornea has fewer sharp edges and the stroma appears in the image as a uniform structure (53).

Figure 12 shows the similarity between the phantom and the cornea. **Taking the phantom into consideration, the refractive index of PMMA ($n=1.4820$) appeared suitable for calibrating the program (91).**

Different geometric characteristics using MATLAB could be calculated. In this study, we present the following values: the steep radius of curvature (s) and the flat radius of curvature (f) for the anterior surface (Ra) (Ra_ s/f) in mm, the steep radius of curvature (s) and the flat radius of curvature (f) for the posterior surface (Rp) (Rp_ s/f) in mm, central corneal thickness (CCT) in μm , the steep surface and flat surface power for the anterior surface (Pa_ s/f) in dpt, the steep surface and flat surface power for the posterior surface (Pp_ s/f) in dpt, the keratometer ($n_C=1.3375$) value for the steep surface (Ks) in dpt, the keratometer ($n_C=1.3375$) value for the flat surface (Kf) in dpt.

All variables in this study were presented by the following values: mean (M), standard deviation (SD), maximum value (Max), minimum value (Min), and the coefficient of variation (CV).

Table 3: The mean (M), standard deviation (SD), maximum (Max), minimum (Min), and coefficient of variation (CV) for each measurement

	Ra_s/f (mm)	Rp_s/f (mm)	CCT (μm)	Pa_s/f (dpt)	Pp_s/f (dpt)	Ks (dpt)	Kf (dpt)
M	7.46/7.67	6.57/6.76	582.0	50.46/49.07	-6.09/-5.92	45.29	44.05
SD	0.24/0.22	0.22/0.21	45.1	1.64/1.35	0.21/0.18	1.47	1.21
Max	7.95/8.80	7.06/7.47	693.9	57.07/53.02	-5.66/-5.35	51.22	47.59
Min	6.59/7.09	5.91/6.18	452.5	47.28/42.74	-6.77/-6.47	42.44	38.36
CV %	3.22/2.87	3.35/3.11	7.75	3.25/2.75	3.45/3.04	3.24	2.75

In our previous published study (53), the data resulted from the analysis of only 74 donor corneas that were compared with the standard eye values according to Gullstrand's model eye in the literature. However, in this study, the average measurements of 200 donor corneas are presented (Table 4).

Table 4: Comparison between the standard eye values according Gullstrand's model eye in literature to the average measurements of the 200 donor corneas (we presented the same comparison in a previous published study, but with a smaller sample size of 74 corneas ^{(adapted and modified (53))}

	Gullstrand's model of the eye	Average measurements of 200 donor corneas	
		Rs	Rf
Ra (mm)	7.7	7.46 ± 0.24	7.67 ± 0.22
Rp (mm)	6.8	6.57 ± 0.22	6.76 ± 0.21
Pa (dpt)	48.83	50.46 ± 1.64	49.07 ± 1.35
Pp (dpt)	-5.88	-6.09 ± 0.21	-5.92 ± 0.18
K (nC=1.3375) (dpt)	42.85	45.29 ± 1.47	44.05 ± 1.21
CCT (µm)	500	582.0 ± 45.1	

Table 5: Different variables with their confidence interval, the number of values outside the confidence interval, and their percentage of data sample (N) (N=200)

Variable name	Confidence interval	Number of values outside the confidence interval /%
The flat radius of curvature for the anterior surface (Ra f)	(7.24-8.09)	6 (3.0%)
The steep radius of curvature for the anterior surface (Ra s)	(6.99-7.92)	7 (3.5%)
The flat radius of curvature for the posterior surface (Rp f)	(6.35-7.16)	11 (5.5%)
The steep radius of curvature for the posterior surface (Rs f)	(6.14-7.01)	4 (2.0%)
Corneal thickness (CCT)	(494.21-670.93)	5 (2.5%)

Abnormalities (beyond ± 2 SD) were found in 13 corneas (6.5%) for anterior surface curvature, 15 for corneas (7.5%) for the posterior surface, and five corneas (2.5%) for thickness (Table 5).

Eleven (5.5%) corneas were not measurable and in seven (3.5%), the brightness of the image captured was high and thus the image could not be analyzed.

4. Discussion

4.1. Modern Eye Banking

The corneal donation process starts usually with obtaining consent from the donor or his/her family. Before the excision of the donor cornea (either the entire globe or just a 15-mm corneoscleral piece of tissue), a detailed past medical and surgical history must be gathered from the family or the donor medical charts to exclude any contraindications such as active meningitis, active hepatitis infection, fungal sepsis, Creutzfeldt-Jakob disease, leukemia, and active disseminated lymphoma. However, medical charts often lack any mention of the donor's ophthalmic history (93, 94).

After excision and placing the donor tissue in an appropriate culture medium, called the "transport medium," a slit lamp examination, microbiological tests, as well as the determination of the endothelial cell density are performed routinely under laboratory conditions in the eye bank (95). However, previous ocular surgeries, such as intrastromal corneal refractive surgery (SMILE), laser photoablation surgery (laser in-situ keratomileusis (LASIK), and photorefractive keratectomy (PRK)), or morphological changes such as subclinical keratoconus, superficial scars, or corneal dystrophies, may be misidentified (96-98).

The increasing popularity of refractive surgery raises concerns about the quality of donor cornea within the eye banking system. Unfortunately, light microscopy and specular microscopy (ECC) alone are inadequate to recognize the history of refractive surgery, e.g., LASIK/ PRK or keratoconus, which causes intraoperative complications and difficulties, such as the LASIK flap coming loose and impairing the visual outcome (99).

Corneas from donors with keratoconus or that had undergone any laser refractive surgery should not be used for PKP because of the diseased corneal stroma layer and, therefore, the unpredictable postoperative refractive result. However, these donors may be eligible for posterior lamellar keratoplasty, such as DMEK (Descemet membrane endothelial keratoplasty) (99).

LASIK and PRK alter the normal anterior corneal architecture through flap creation, tissue ablation, or both. However, these changes may have been beneficial for living patients. Such a donor cornea with a history of prior refractive procedure has the risk of irregular astigmatism, induced hyperopia, and possible flap dehiscence in the recipient (100, 101). There are a few

cases in the literature in which donor corneas with different types of refractive surgery have been unintentionally transplanted into patients undetected (102,103). Kang et al. (98) showed that up to 10% of corneas in eye banks may have undergone an unidentified LASIK procedure.

Clear cornea cataract wounds, astigmatic keratotomy scars, and arcus senilis changes can mimic a LASIK flap to an inexperienced slit-lamp observer (104). Moreover, the reliability is limited by postmortem changes, such as severe epithelial edema, corneal erosion with stromal edema, and hypotonia. Therefore, new screening methods with increasing specificity and sensitivity are required to avoid any unwanted intraoperative or postoperative results (105).

4.2. Detection of curvature abnormalities in the donor

Placido disk videokeratography has been proposed as an evaluation method to detect curvature abnormalities in donors (106). Hereby, curvature deviation of the front surface can be recognized. However, this method does not allow for further analysis of the stromal tissue or the corneal thickness. Moreover, this method requires artificially increasing the intraocular pressure for good topographic reading and is, therefore, limited to whole eyes rather than corneoscleral discs and is highly sensitive to the corneal epithelium's quality (Figure 13) (107).



Figure 13: A videokeratoscope presented by Stoiber et al. as an evaluation method to screen the donor tissues (adapted and modified (107))

Terry et al. (97) presented an evaluation method to examine the donor corneas (Orbscan, Bausch & Lomb, Rochester, NY, USA). Herein, the curvature and the pachymetry could be assessed. However, eye banks perform mostly the corneoscleral technique, which makes this method limited and thus not being suitable for all eye banks.

In addition, both techniques require mounting the cornea in the air, which comes with increased risk of contamination, impaired sterility conditions, and risk of damage to the epithelium, including drying and sloughing of cells (97, 106).

OCT has been proposed as a suitable method for donor cornea screening because of its high resolution and because it allows for sterile, direct, noncontact tomographic imaging of corneal donor tissue with the donor tissue placed within the culture flask (52, 105).

First attempts have been proposed by Neubauer and Priglinger using a time-domain OCT (107). Lin (108) developed a laboratory system to perform corneal screening in a viewing

chamber using a custom-made high-resolution laser source and monitoring refractive index distributions to differentiate between normal corneas and LASIK-operated corneas. In a different study, Lin et al. (109) presented a technique for defining LASIK-operated corneas by measuring the anterior curvature and the anterior/posterior stromal reflectivity ratio with OCT scans.

Keratoconus and post-refractive surgery corneas could be detected by analyzing the anterior and posterior radii of curvature and the corneal thickness profile or by detecting structural changes in the corneal tissue (105). Therefore, OCT use as a screening method has been improved with different devices and methods by Janunts et al. (110), who presented the use of swept-source OCT (CASIA SS-1000, Tomey Corp., Nagoya, Japan), and Damian et al. (52), who presented the use of spectral-domain OCT (Spectralis Anterior Segment Module, Heidelberg Engineering GmbH, Heidelberg, Germany).

In our study, a swept-source AS-OCT was used (CASIA 2 (Tomey Corp., Nagoya, Japan)). CASIA 2 has advantages over the previous OCT devices in different aspects including the range of measurement and the resolution. The time-domain OCT has a smaller range of measurement and a lower resolution (108).

Damian et al. (52) used the spectral 2 OCT (Heidelberg Engineering, Heidelberg, Germany) and reached by an image pickup of a maximum lateral diameter of 8.3 mm and 1.9 mm axial, a measuring range of 5 mm x 5 mm at a lateral resolution of about 11 μm , and an axial resolution of 3.9 μm . However, with AS-OCT CASIA 2, which was used in this study, a lateral diameter of up to 16 mm can be recorded at a depth of up to 13 mm, thus allowing a larger measurement range of the cornea of 7 mm \times 7 mm. The large depth measurement range of up to 13 mm allows for complete uptake of the donor corneas within the culture flask and, in the end, after processing the collected data using a special program (MATLAB), a 3D

volume of the donor cornea can be achieved. Therefore, CASIA 2 shows significant improvement in measuring range and the sterility conditions during measurement (53). Moreover, the position of the printed holder during the measurement makes it simpler to use the OCT as a routine screening method for everyday use (26).

In the present study, abnormalities were found in 13 corneas for the anterior surface, 15 corneas for the posterior surface, and five corneas for thickness, which indicates the ability to identify corneas with thickness or refractive abnormalities, which cannot be used for penetrating keratoplasty but are still eligible for DMEK or DSAEK. Therefore, the corneal donor selection can be optimized under the everyday eye bank condition. In the future, this technique may allow for the ‘harmonization’ of donor and host tomography to improve corneal astigmatism after keratoplasty.

4.3. Limitations of the present study

1) The measurement was carried out about 24 hours after placing the donor corneas in medium 2, which includes 6% dextran T-500. Schnitzler et al. suggested that the minimum corneal thickness was reached after 24 hours (111). However, the culture medium in their study differed somewhat from what we used in our study. Therefore, the actual time between placing the corneas in the culture medium and the measurement can be one of this study's limitations. In a new study of our group, donor corneas are examined with AS-OCT hourly for 24 hours to determine the time required for deswelling (112). At this time, it seems that a superficial deswelling is reached even after 12 hours in medium 2.

2) Another limitation of our study is that the true values of the corneal curvature and thickness of donor corneas are not known and donor corneas were measured in a flask fixed in a holder, which means there was a risk to cause a slight defect in the donor cornea before the measurement. However, there was no comparison with the in-situ geometry available. Therefore, we could only refer to literature values for comparison (53) (Table 4).

3) Moreover, regardless of the highly qualified team we had in this study, we cannot exclude the risk of human error in the harvesting and storage process. However, further studies are required to be able to exclude any specific pathologies or human error in the process.

4) AS-OCT provides a new sterile screening method to identify corneal morphological and refractive alterations. However, further studies with a larger sample size in the future are required to identify a specific diagnosis or a specific pathology. Nevertheless, many morphological pathologies can already be detected by the experienced routine use of slit lamps in the eye bank.

4.3. Conclusions

The AS-OCT provides an objective, sterile and may allow in the future a semi-automated screening method to identify corneal morphological and refractive alterations (e.g., keratoconus, status post PRK/LASIK) to optimize corneal donor selection in eye banks. To surely avoid refractive surprises after corneal transplantation, abnormal donor corneas can easily be used for DMEK or DSAEK instead of penetrating keratoplasty or DMEK.

5. References

- (1) Crawford AZ, Patel DV, Mc Ghee CNJ. A brief history of corneal transplantation: From ancient to modern. *Oman J Ophthalmol* 2013;6:12–17.
- (2) Moffatt SL, Cartwright VA, Stumpf TH. Centennial review of corneal transplantation. *Clin Experiment Ophthalmol* 2005;33:642–657.
- (3) Zirm E. [A successful total keratoplasty]. *Arch Ophthalmol* 1906;64:580–593.
- (4) Filatov V. Transplantation of the cornea from preserved cadavers' eyes. *Lancet* 1937;1:1395–1397.
- (5) Tan DT, Dart JK, Holland EJ, Kinoshita S. Corneal transplantation. *Lancet* 2012;379:1749-1761.
- (6) Paton D. The founder of the first eye bank: R. Townley Paton, MD. *Refract Corneal Surg* 1991;7:190–195.
- (7) Castroviejo R. Keratoplasty. *Am J Ophthalmol* 1941;24:1–20.
- (8) Polack FM. Ramon Castroviejo 1904-1987. *Cornea* 2000;19:593–602.
- (9) Cassidy D, Sharma N, Vajpayee RB. Evolution of endothelial keratoplasty. New Delhi: Jaypee Highlights Medical Publishers, Inc.; 2013.
- (10) Boynton GE, Woodward MA. Evolving techniques in corneal transplantation. *Curr Surg Rep* 2015;3:2.
- (11) Seitz B, Szentmáry N, Langenbucher A, Hager T, Viestenz A, Janunts E, El-Husseiny M. [PKP for keratoconus – from hand/motor trephine to excimer laser and back to femtosecond laser]. *Klin Monatsbl Augenheilkd* 2016;233:727-736.
- (12) Seitz B, Cursiefen C, El-Husseiny M, Viestenz A, Langenbucher A, Szentmáry N. [DALK and penetrating laser keratoplasty for advanced keratoconus]. *Ophthalmologe* 2013;110:839–848.
- (13) Luengo-Gimeno F, Tan DT, Mehta JS. Evolution of deep anterior lamellar keratoplasty (DALK). *Ocul Surf* 2011;9:98-110.
- (14) Keenan TD, Carley F, Yeates D, Jones MN, Rushton S, Goldacre MJ; NHSBT Ocular Tissue Advisory Group and contributing ophthalmologists (OTAG Audit Study 8). Trends in corneal graft surgery in the UK. *Br J Ophthalmol* 2011;95:468-472.
- (15) Seitz B, Lisch W, Weiss J. [The revised newest IC3D classification of corneal dystrophies]. *Klin Monatsbl Augenheilkd* 2015;232:283–294.
- (16) Tillett CW. Posterior lamellar keratoplasty. *Am J Ophthalmol* 1956;41:530–533.

- (17) Polack FM, Smelser GK, Rose J. Long-term survival of isotopically labeled stromal and endothelial cells of corneal homografts. *Am J Ophthalmol* 1964;57:67–78.
- (18) Culbertson WW. Endothelial replacement: flap approach. *Ophthalmol Clin North Am* 2003;16:113–118.
- (19) Melles GR, Eggink FA, Lander F, Pels E, Rietveld FJ, Beekhuis WH, Binder PS. A surgical technique for posterior lamellar keratoplasty. *Cornea* 1998;17:618–626.
- (20) Melles GR, Lander F, Beekhuis WH, Remeijer L, Binder PS. Posterior lamellar keratoplasty for a case of pseudophakic bullous keratopathy. *Am J Ophthalmol* 1999;127:340–341.
- (21) Terry MA, Ousley PJ. Endothelial replacement without surface corneal incisions or sutures: topography of the deep lamellar endothelial keratoplasty procedure. *Cornea* 2001;20:14–18.
- (22) Terry MA. Endothelial keratoplasty: history, current state and future directions. *Cornea* 2006;25:873-878.
- (23) Anshu A, Price MO, Tan DT, Price FW Jr. Endothelial keratoplasty: a revolution in evolution. *Surv Ophthalmol* 2012;57:236–252.
- (24) Price FW Jr, Price MO. Evolution of endothelial keratoplasty. *Cornea* 2013;32:28-32.
- (25) Lee WB, Jacobs DS, Musch DC, Kaufman SC, Reinhart WJ, Shtein RM. Descemet's stripping endothelial keratoplasty: safety and outcomes: a report by the American Academy of Ophthalmology. *Ophthalmology* 2009;116:818-1830.
- (26) Flockerzi E, Maier P, Böhringer D, Reinshagen H, Kruse F, Cursiefen C, Reinhard T, Geerling G, Torun N, Seitz B; all German Keratoplasty Registry Contributors. Trends in Corneal Transplantation from 2001 to 2016 in Germany: A Report of the DOG-Section Cornea and its Keratoplasty Registry. *Am J Ophthalmol* 2018;188:91-98.
- (27) Ponzin D, Salvalaio G, Ruzza A, Parekh M, Ferrari S. Development in corneal Banking. In: Hjortdal J. *Corneal Transplantation*. Springer Heidelberg, New York, Dordrecht, London 2016:27-29.
- (28) Armitage WJ, Tullo AB, Larkin DFP. The first successful full-thickness corneal transplant: a commentary on Eduard Zirm's landmark paper of 1906. *Br J Ophthalmol* 2006;90:1222-1223
- (29) Filatov VP, Sitchevska O. Transplantation of the cornea. *Arch Ophthalmol* 1935;13:321-347.

- (30) Armitage WJ. Preservation of human cornea. *Transfus Med Hemother* 2011;38:143-147.
- (31) Pels L. Organ culture: the method of choice for preservation of human donor corneas. *Br J Ophthalmol* 1997;81:523–525.
- (32) Stocker FW. The endothelium of the cornea and its clinical implications. *Trans Am Ophthalmol Soc* 1953;51:669–786.
- (33) McCarey BE, Kaufman HE. Improved corneal storage. *Invest Ophthalmol Vis Sci* 1974;13:165–173.
- (34) Bigar F, Kaufman HE, McCarey BE, Binder PS. Improved corneal storage for penetrating keratoplasties in man. *Am J Ophthalmol* 1975;79:115–120.
- (35) Doughman DJ, Van Horn D, Harris JE, Miller GE, Lindstrom R, Good RA. The ultrastructure of human organ-cultured cornea. I. Endothelium. *Arch Ophthalmol* 1974;92:516–523.
- (36) Summerlin WT, Miller GE, Harris JE, Good RA. The organ-cultured cornea: an in vitro study. *Invest Ophthalmol* 1973;12:176–180.
- (37) Doughman DJ, Harris JE, Schmidt KM. Penetrating keratoplasty using 37°C organ-cultured cornea. *Trans Sect Ophthalmol Am Acad Ophthalmol Otolaryngol* 1976;81:778–793.
- (38) Brunette I, Le Francois M, Tremblay MC, Guertin MC. Corneal transplant tolerance of cryopreservation. *Cornea* 2001;20:590-596.
- (39) Fuller BJ: The effect of cooling on mammalian cells; in Fuller BJ, Court BWW (eds): *Clinical applications of cryobiology*. Boca Raton, CRC Press, 1991:1-22.
- (40) Kuwahara Y, Sakanoue M. Preservation of donor eyes for penetrating keratoplasty (regarding medium term preservation). *Nippon Ganka Kyo* 1968;19:1319-1327.
- (41) Pels E, Schuchard Y. Organ culture and endothelial evaluation as a preservation method for human corneas. In: Brightbill FS, ed. *Corneal surgery*. 2nd ed. St Louis: Mosby, 1986:93–102.
- (42) Borderie V, Scheer S, Touzeau O, Védie F, Carvajal-Gonzalez S, Laroche L. Donor organ cultured corneal tissue selection before penetrating keratoplasty. *Br J Ophthalmol* 1998;82:382-388.
- (43) Claerhout I, Maas H, Pels E: *European Eye Bank Association Directory Report*, 18th ed. 2010. www.europaneyebanks.org.

- (44) Abdin A, Daas L, Pattmüller M, Suffo S, Langenbucher A, Seitz B. Negative impact of Dextran in organ culture media for pre-stripped tissue preservation on DMEK (Descemet Membrane Endothelial Keratoplasty) outcome. *Graefes Arch Clin Exp Ophthalmol* 2018;256:2135-2142.
- (45) Musch DC, Meyer RF, Sugar A. Predictive factors for endothelial cell loss after penetrating keratoplasty. *Arch Ophthalmol* 1993;111:80-83.
- (46) Cornea Donor Study Investigator Group, Gal RL, Dontchev M, Beck RW, Mannis MJ, Holland EJ, Kollman C, Dunn SP, Heck EL, Lass JH, Montoya MM, Schultze RL, Stulting RD, Sugar A, Sugar J, Tennant B, Verdier DD. The effect of donor age on corneal transplantation outcome results of the cornea donor study. *Ophthalmology* 2008;115:620-626.
- (47) Armitage WJ, Dick AD, Bourne WM. Predicting endothelial cell loss and long-term corneal graft survival. *Invest Ophthalmol Vis Sci* 2003;44:3326-3331.
- (48) Wiffen SJ, Nelson LR, Ali AF, Bourne WM. Morphologic assessment of corneal endothelium by specular microscopy in evaluation of donor corneas for transplantation. *Cornea* 1995;14:554–561.
- (49) Rand GM, Kwon JW, Gore PK, McCartney MD, Chuck RS. Technician consistency in specular microscopy measurements: a “Real-World” retrospective analysis of a United States Eye Bank. *Cornea* 2017;36:1172-1177.
- (50) Lass JH, Gal RL, Ruedy KJ, Benetz BA, Beck RW, Baratz KH, Holland EJ, Kalajian A, Kollman C, Manning FJ, Mannis MJ, McCoy K, Montoya M, Stulting D, Xing D; Cornea Donor Study Group. An evaluation of image quality and accuracy of eye bank measurement of donor cornea endothelial cell density in the Specular Microscopy Ancillary Study. *Ophthalmology* 2005;112:431-440.
- (51) 2016 Eye Banking Statistical Report. Washington, DC: Eye Bank Association of America; 2017.
- (52) Damian A, Seitz B, Langenbucher A, Eppig T. Optical coherence tomography-based topography determination of corneal grafts in eye bank cultivation. *J Biomed Opt* 2017;22:16001.
- (53) Mäurer S, Asi F, Rawer A, Damian A, Seitz B, Langenbucher A, Eppig T. [Concept for 3D measurement of corneal donor tissue using a clinical OCT]. *Ophthalmologe* 2019;116:640-646.

- (54) Huang D, Swanson EA, Lin CP, Schuman JS, Stinson WG, Chang W, Hee MR, Flotte T, Gregory K, Puliafito CA and Fujimoto JG. Optical coherence tomography. *Science* 1991;254:1178-1181.
- (55) Jancevski M, Foster CS. Anterior segment optical coherence tomography. *Semin Ophthalmol* 2010;25:317-323.
- (56) Hirano K, Yasuki I, Suzuki T, Kojima T, Kachi S, Miyake Y. Optical coherence tomography for the noninvasive evaluation of the cornea. *Cornea* 2001;20:281-289.
- (57) Fante RJ, Shtein RM, Titus MS, Woodward MA. Anterior segment optical coherence tomography versus ultrasound pachymetry to measure corneal thickness in endothelial keratoplasty donor corneas. *Cornea* 2013;32:79-82.
- (58) Ramos JIB, Li Y, Huang D. Clinical and research applications of anterior segment optical coherence tomography - a review. *Clin Exp Ophthalmol* 2009;37:81-89.
- (59) Izatt JA, Hee MR, Swanson EA, Lin CP, Huang D, Schuman JS, Puliafito CA, Fujimoto JG. Micrometer-scale resolution imaging of the anterior eye in vivo with optical coherence tomography. *Arch Ophthalmol* 1994;112:1584-1589.
- (60) Radhakrishnan S, Rollins AM, Roth JE, Yazdanfar S, Westphal V, Bardenstein DS, Izatt JA. Real-time optical coherence tomography of the anterior segment at 1310 nm. *Arch Ophthalmol* 2001;1179-1185.
- (61) Brown JS, Wang D, Li X, Baluyot F, Iliakis B, Lindquist TD, Shirakawa R, Shen TT, Li X. In situ ultrahigh-resolution optical coherence tomography characterization of eye bank corneal tissue processed for lamellar keratoplasty. *Cornea* 2008;27:802-810.
- (62) Han SB, Liu YC, Noriega KM, Mehta JS. Applications of anterior segment optical coherence tomography in corneal and ocular surface disease. *J Ophthalmol* 2016;4971572. Epub 2016 Sep 19.
- (63) Vajzovic LM, Karp CL, Haft P, Shousha MA, Dubovy SR, Hurmeric V, Yoo SH, Wang J. Ultra high-resolution anterior segment optical coherence tomography in the evaluation of anterior corneal dystrophies and degenerations. *Ophthalmology* 2011;118:1291-1296.
- (64) Thomas BJ, Galor A, Nanji AA, El Sayyad F, Wang J, Dubovy SR, Joag MG, Karp CL. Ultra high-resolution anterior segment optical coherence tomography in the diagnosis and management of ocular surface squamous neoplasia. *Ocul Surf* 2014;12:46-58.

- (65) Gumus K, Crockett CH, Pflugfelder SC. Anterior segment optical coherence tomography: a diagnostic instrument for conjunctivochalasis. *Am J Ophthalmol* 2010;150:798-806.
- (66) Nanji AA, Sayyad FE, Galor A, Dubovy S, Karp CL. High-resolution optical coherence tomography as an adjunctive tool in the diagnosis of corneal and conjunctival pathology. *Ocul Surf* 2015;13:226-235.
- (67) Soliman W, Mohamed TA. Spectral domain anterior segment optical coherence tomography assessment of pterygium and pinguecula. *Acta Ophthalmol* 2012;90:461-465.
- (68) Krema H, Santiago RA, Gonzalez JE, Pavlin CJ. Spectral-domain optical coherence tomography versus ultrasound biomicroscopy for imaging of nonpigmented iris tumors. *Am J Ophthalmol* 2013;156:806-812.
- (69) Hau SC, Papastefanou V, Shah S, Sahoo MS, Restori M, Cohen V. Evaluation of iris and iridociliary body lesions with anterior segment optical coherence tomography versus ultrasound B-scan. *Br J Ophthalmol* 2015;99:81-86.
- (70) Jung SH, Han KE, Stulting RD, Sgrignoli B, Kim TI, Kim EK. Phototherapeutic keratectomy in diffuse stromal haze in granular corneal dystrophy type 2. *Cornea* 2013;32:296-300.
- (71) Konstantopoulos A, Kuo J, Anderson D, Hossain P. Assessment of the use of anterior segment optical coherence tomography in microbial keratitis. *Am J Ophthalmol* 2008;146:534-542.
- (72) Vanathi M, Behera G, Vengayil S, Panda A, Khokhar S. Intracameral SF6 injection and anterior segment OCT-based documentation for acute hydrops management in pellucid marginal corneal degeneration. *Cont Lens Anterior Eye* 2008;31:164-166.
- (73) Khurana RN, Li Y, Tang M, Lai MM, Huang D. Highspeed optical coherence tomography of corneal opacities. *Ophthalmology* 2007;114:1278-1285.
- (74) Agarwal A, Ashokkumar D, Jacob S, Agarwal A, Saravanan Y. High-speed optical coherence tomography for imaging anterior chamber inflammatory reaction in uveitis: clinical correlation and grading. *Am J Ophthalmol* 2009;147:413-416.
- (75) Ibrahim OM, Dogru M, Takano Y, Satake Y, Wakamatsu TH, Fukagawa K, Tsubota K, Fujishima H. Application of Visante optical coherence tomography tear meniscus height measurement in the diagnosis of dry eye disease. *Ophthalmology* 2010;117:1923-1929.

- (76) Zhou S, Li Y, Lu AT, Liu P, Tang M, Yiu SC, Huang D. Reproducibility of tear meniscus measurement by Fourier-domain optical coherence tomography: a pilot study. *Ophthalmic Surg Lasers Imaging* 2009;40:442-447.
- (77) Nguyen P, Huang D, Li Y, Sadda SR, Ramos S, Pappuru RR, Yiu SC. Correlation between optical coherence tomography-derived assessments of lower tear meniscus parameters and clinical features of dry eye disease. *Cornea* 2012;31:680-685.
- (78) Akiyama R, Usui T, Yamagami S. Diagnosis of dry eye by tear meniscus measurements using anterior segment swept source optical coherence tomography. *Cornea* 2015;34:115-120.
- (79) Qiu X, Gong L, Sun X, Jin H. Age-related variations of human tear meniscus and diagnosis of dry eye with Fourier-domain anterior segment optical coherence tomography. *Cornea* 2011;30:543-549.
- (80) Wylegala E, Dobrowolski D, Nowińska A, Tarnawska D. Anterior segment optical coherence tomography in eye injuries. *Graefe's Arch Clin Exp Ophthalmol* 2009;4:451-455.
- (81) Ryan DS, Sia RK, Colyer M, Stutzman RD, Wroblewski KJ, Mines MJ, Bower KS. Anterior segment imaging in combat ocular trauma. *J Ophthalmol* 2013;Article ID 308259:8 pages.
- (82) Nguyen P, Chopra V. Applications of optical coherence tomography in cataract surgery. *Curr Opin Ophthalmol* 2013;24:47-52.
- (83) Tang M, Wang L, Koch DD, Li Y, Huang D. Intraocular lens power calculation after previous myopic laser vision correction based on corneal power measured by Fourier domain optical coherence tomography. *J Cataract Refract Surg* 2012;38:589-594.
- (84) Choi CY, Youm DJ, Kim MJ, Tchah H. Changes in central corneal thickness of preserved corneas over time measured using anterior segment optical coherence tomography. *Cornea* 2009;28:536-540.
- (85) Amato D, Lombardo M, Oddone F, Nubile M, Colabelli Gisoldi RA, Villani CM, Yoo S, Parel JM, Pocobelli A. Evaluation of a new method for the measurement of corneal thickness in eye bank posterior corneal lenticules using anterior segment optical coherence tomography. *Br J Ophthalmol* 2011;95:580-584.
- (86) Li Y, Netto MV, Shekhar R, Krueger RR, Huang D. A longitudinal study of LASIK flap and stromal thickness with high-speed optical coherence tomography. *Ophthalmology* 2007;114:1124-1132.

- (87) Rosas Salaroli CH, Li Y, Zhang X, Tang M, Branco Ramos JL, Allemann N, Huang D. Repeatability of laser in situ keratomileusis flap thickness measurement by Fourier domain optical coherence tomography. *J Cataract Refract Surg* 2011;37:649-654.
- (88) Rocha KM, Perez-Straziota CE, Stulting RD, Randleman JB. Epithelial and stromal remodeling after corneal collagen cross-linking evaluated by spectral-domain OCT. *J Refract Surg* 2014;30:122-127.
- (89) Rio-Cristobal A, Martin R. Corneal assessment technologies: current status. *Surv Ophthalmol* 2014;59:599-614.
- (90) Zhang Q, Jin W, Wang Q. Repeatability, reproducibility, and agreement of central anterior chamber depth measurements in pseudophakic and phakic eyes: optical coherence tomography versus ultrasound biomicroscopy. *J Cataract Refract Surg* 2010;36:941-946.
- (91) Eppig T, Mäurer S, Daas L, Seitz B, Langenbucher A. Imaging the Cornea, Anterior Chamber and Lens in Corneal and Refractive Surgery. In: Lanza M (Hrsg) *Clinical Application of OCT in Ophthalmology* 2018: 133-152.
- (92) Beadie G, Brindza M, Flynn RA, Rosenberg A, Shirk JS. Refractive index measurements of polymethyl methacrylate (PMMA) from 0.4–1.6 μm . *Appl Opt* 2015;54:139-143.
- (93) Terry MA, Ousley PJ, Rich LF, Wilson DJ. Evaluation of prior photorefractive keratectomy in donor tissue. *Cornea* 1999;18:353-358.
- (94) Mannis MJ, McDonough G, Howard K, Morales R, Sugar J. Screening donor corneas the have undergone PRK. *Cornea* 1997;16:683-685.
- (95) Borderie V, Martinache C, Sabolic V, Touzeau O, Laroche L. Light microscopic evaluation of human donor corneal stroma during organ culture. *Acta Ophthalmol Scand* 1998;76:154-157.
- (96) Laliberté JF, Meunier J, Hick S, Brunette I; Canadian Refractive Surgery Research Group. Topography-based screening for previous laser in situ keratomileusis to correct myopia and hyperopia. *Cornea* 2015;24:167-177.
- (97) Terry MA, Ousley PJ. New screening methods for donor eye-bank eyes. *Cornea* 1999;18:430-436.
- (98) Kang SJ, Schmack I, Edelhauser HF, Grossniklaus HE. Donor cornea misidentified with prior laser in situ keratomileusis. *Cornea* 2010;29:670-673.

- (99) Fargione RA, Channa P. Cornea donors who have had prior refractive surgery: data from the Eye Bank Association of America. *Curr Opin Ophthalmol* 2016;27:323-326.
- (100) Ousley PJ1, Terry MA. Objective screening methods for prior refractive surgery in donor tissue. *Cornea* 2002;21:181-188.
- (101) Angulo EM. Accidental grafting of a donor cornea with radial keratotomy in a keratoconus patient. *J Refract Corneal Surg* 1989;5:198.
- (102) Adi MC, Caron AL, Fides RNC, David RS. Two cases of a LASIK surgery. *Cornea* 2002;21:111-113.
- (103) Mootha VV, Dawson D, Kumar A, Gleiser J, Qualls C, Albert DM. Slitlamp, specular, and light microscopic findings of human donor corneas after laser-assisted in situ keratomileusis. *Arch Ophthalmol* 2004;122:686–692
- (104) Wolf AH, Neubauer AS, Priglinger SG, Kampik A, Welge-Luessen UC. Detection of laser in situ keratomileusis in a postmortem eye using optical coherence tomography. *J Cataract Refract Surg* 2004;30:491-495.
- (105) Lim-Bon-Siong R, Williams JM, Samapunphong S, Chuck RS, Pepose JS. Screening of myopic photorefractive keratectomy in eye bank eyes by computerized videokeratography. *Arch Ophthalmol* 1998;116:617-623.
- (106) Stoiber J, Ruckhofer J, Hitzl W, Grabner G. Evaluation of donor tissues with a new videokeratoscope - the Keraton Scout. *Cornea* 2001;20:859-863.
- (107) Priglinger SG, Neubauer AS, May CA, Alge CS, Wolf AH, Mueller A, Ludwig K, Kampik A, Welge-Luessen U. Optical coherence tomography for the detection of laser in situ keratomileusis in donor corneas. *Cornea* 2003;22:46-50.
- (108) Lin RC. Optical coherence tomography for the screening of donor corneas and examination of the retinal nerve fiber directional reflectance [dissertation]. Case western reserve university;2006,p46.
- (109) Lin RC, Li Y, Tang M, McLain M, Rollins AM, Izatt JA, Huang D. Screening for previous refractive surgery in eye bank corneas by using optical coherence tomography. *Cornea* 2007;26:594-599.
- (110) Janunts E, Langenbacher A, Seitz B. In vitro corneal tomography of donor cornea using anterior segment OCT. *Cornea* 2016;35:647–653.
- (111) Schnitzler AC, Salla S, Hamsley N, Flammersfeld A, Fuest M, Walter P, Hermel M. Role of the endothelial layer in the deswelling process of organ-cultured human corneas before transplantation. *Cornea* 2016;35:1216–1221.

(112) Hamon L, Daas L, Mäurer S, Schulz K, Asi F, Langenbucher A, Seitz B: Kinetics of the deswelling process of corneal grafts with dextran-containing culture medium before keratoplasty. Tagung der Association for Research in Vision and Ophthalmology (ARVO), Vancouver, Kanada, 28.04.-02.05.2019.

Acknowledgments

I am deeply thankful to my beloved husband, whom my words would be never enough to describe. I could not wish for greater support, love, and understanding. In addition, to my parents and my brothers who are continually inspirational and have enabled me to have such a wonderful education and taught me to follow my dreams, I am forever grateful. This thesis is for all of you.

I would like to express my deep and sincere gratitude to my research supervisor, Dr. Berthold Seitz, Professor and Chief of the Ophthalmology Department, Saarland University, Homburg, for giving me the opportunity to do this research and his continued guidance, inspiration, advice, and support throughout this project.

Special thanks go to Dr. Alaa-din Abdin for his support and guidance to complete my dissertation successfully.

I am very thankful to the Experimental Ophthalmology Department, Saarland University, for their support and guidance. Special thanks go to Ms. Mäurer for her effort in analyzing the data captured with AS-OCT; I wish her the best success with her dissertation.

I also confirm my gratitude to my colleagues at the LIONS-Eye Bank for their support, especially in the methodology part.

Special thanks to my beloved brother Dr. Khalid Asi, for his great professional and emotional support. Thank you for always being there.

Last but not least, thanks go to all the donor patients without whom this thesis and much other research would not have been completed.

**Aus datenschutzrechtlichen Gründen wird der Lebenslauf in der elektronischen
Fassung der Dissertation nicht veröffentlicht.**

Aus datenschutzrechtlichen Gründen wird der Lebenslauf in der elektronischen Fassung der Dissertation nicht veröffentlicht.

Tag der Promotion: 11. November 2020

**Dekan: Univ.-Prof. Dr. med. Michael D.
Menger**

**Berichterstatter: Prof. Dr. Berthold Seitz
Prof. Dr. Henning Madry**